VIA MEDICA

ORIGINAL ARTICLE

Yonghu Song*, Jianhui Li*, Zhenyang Lu, Yijun Qi

Department of General Surgery, The First Affiliated Hospital of Anhui Medical University, Anhui, China
These authors contributed equally

ARPC3 affects the prognosis for patients with hepatocellular carcinoma by regulating the immune response

Address for correspondence:
Prof. Yijun Qi, PhD
Department of General Surgery,
The First Affiliated Hospital
of Anhui Medical University,
Hefei 230022, Anhui, China
e-mail: qiyijun8446@sina.com

Oncology in Clinical Practice
DOI: 10.5603/ocp.99819

ISSN 2450–1654
e-ISSN 2450–6478

ABSTRACT

Introduction. Actin related protein 2/3 complex subunit 3 (*ARPC3*) is associated with a poor prognosis in patients with various cancers. However, the mechanisms by which it affects immunotherapy and prognosis in patients with hepatocellular carcinoma (HCC) remain unclear.

To explore the effect of *ARPC3* on immune checkpoint inhibitors (ICIs), we investigated the association of *ARPC3* with immunotherapy-associated ferroptosis genes.

Material and methods. The expression difference in *ARPC3* between normal and HCC tissues and the effect of *ARPC3* on prognosis were evaluated by using multiple databases. GSEA was used to predict the pathway by which *ARPC3* affects HCC progression. Using the TCGA database, the First Affiliated Hospital of Anhui Medical University (AHMU) database, and the ICGC database, the correlation between *ARPC3*, tumor-infiltrating lymphocytes (TILs) and immune checkpoints was studied.

Results. The expression of *ARPC3* in normal tissues was lower than that in tumor tissues, and as an independent prognostic risk factor for HCC, patients with HCC whose *ARPC3* expression was high had a worse prognosis. GSEA suggested that the upregulation of *ARPC3* mainly affected immune-related pathways. Three databases showed that *ARPC3* expression levels affected the infiltration levels of B cells, T cells, macrophages, neutrophils, and NK cells in tumors. In addition, we confirmed that *ARPC3* may influence the efficacy of ICI therapy by affecting the expression of immune checkpoints and ferroptosis-related genes in HCC.

Conclusions. *ARPC3* is an independent prognostic risk factor for HCC patients and may influence HCC immunotherapy by affecting the expression of immune checkpoints and ferroptosis-related genes.

Keywords: *ARPC3*, hepatocellular carcinoma, prognosis, biomarker, immunotherapy

Oncol Clin Pract

Introduction

Primary liver cancer is one of the most common cancers, and 80-90% of cases are hepatocellular carcinoma (HCC) [1]. According to global cancer statistics, liver cancer had the sixth highest incidence and the second highest mortality in 2020, with 50% of cases deriving from China [2]. Currently, the dominant therapy for HCC patients is still liver resection, but the surgical resection rate of HCC is still low [3, 4]. With the development and application of neoadjuvant therapy in recent years, the resection rate of liver cancer has improved, and the recurrence rate has been reduced. Therefore, many patients with advanced HCC have benefited from the combined application of immune checkpoint inhibitors (ICIs) and targeted drugs in clinical treatment, but the objective response rate (ORR) is still low for HCC patients receiving immunotherapy and targeted therapy, and drug resistance is increasing, which remains a challenge in the treatment of this disease [5]. The tumor microenvironment (TME) mainly comprises tumor cells, immune cells, stromal cells, and other components [6]. Immunotherapy is not affected by mutation and drug resistance, which significantly reduces the metastatic ability of tumor cells [6]. Based on accumulating evidence, tumor-infiltrating lymphocytes (TILs) impact the outcome and effectiveness of

Received: 16.03.2024 Accepted: 05.05.2024 Early publication: 11.06.2024

immunotherapy in patients with malignant tumors [7–9]. For example, TIL expression is positively correlated with better prognosis and higher ORR to ICIs in patients with gastric cancer, HCC, breast carcinoma, nasopharyngeal cancer, non-small cell lung cancer, etc. [10–14]. Therefore, the identification of new immune-related biomarkers, potential drug targets, and genes associated with TILs is important.

The actin cytoskeleton is involved in a wide variety of cellular functions that affect the activity, migration, and invasion of tumor cells [15, 16]. The actin-related 2/3 protein (ARP2/3) consists of 2 actin-related proteins (ARP2 and ARP3) and 5 protein subunits (*ARPC1* to *ARPC5*). At present, the biological functions of ARP2/3 have been extensively studied [17–19]. For instance, *ARPC3* knockdown significantly inhibits the migration of the colon cancer cell line HT29 [20, 21], suggesting that *ARPC3* may be a key factor regulating tumor cell migration and invasion. The function of *ARPC3* in HCC is still obscure, especially in immunology.

The research design of this study is shown in the flowchart (Fig. 1).

Material and methods

First Affiliated Hospital of Anhui Medical University hepatocellular carcinoma sample collection and follow-up

In this study, 60 HCC patients who underwent surgical resection at First Affiliated Hospital of Anhui Medical University (AHMU) in 2017 were randomly selected. Tumor diameter, tumor number, hepatitis B virus surface antigen (HBsAg), and alpha-fetoprotein (AFP) levels were included in univariate and multivariate studies. The research was performed in accordance with the 1964 Declaration of Helsinki. In addition, the study was approved by the AHMU Ethics Committee.

RNA extraction and measurement of gene expression

RNA was extracted from all HCC and paracancerous tissue samples using TRIzol (AG21101, Accurate Biotechnology, China). According to the manufacturer's instructions, RNA was reverse transcribed to cDNA (AG11706, Accurate Biotechnology, China). Using cDNA templates, gene expression levels in HCC were explored using qRT-PCR with primers specific for *ARPC3, GAPDH, PD-1, PD-L1, PD-L2, CTLA4, IDO1*, and *TNFRSF14*. The $2^{-\Delta\Delta Ct}$ method and *GAPDH* as an internal control were used to calculate the relative expression level. The cutoff value [(sensitivity + specificity) −1] was calculated by drawing a receiver operating characteristic (ROC) curve, and *ARPC3* was divided into high- and low-expression groups. The primer sequences used in our research are listed in Table 1.

Public dataset download and validation

The Cancer Genome Atlas (TCGA) (https://tcga-data.nci.nih.gov/docs/publications/tcga/) and the International Cancer Genome Consortium (ICGC; https://dcc.icgc.org/)

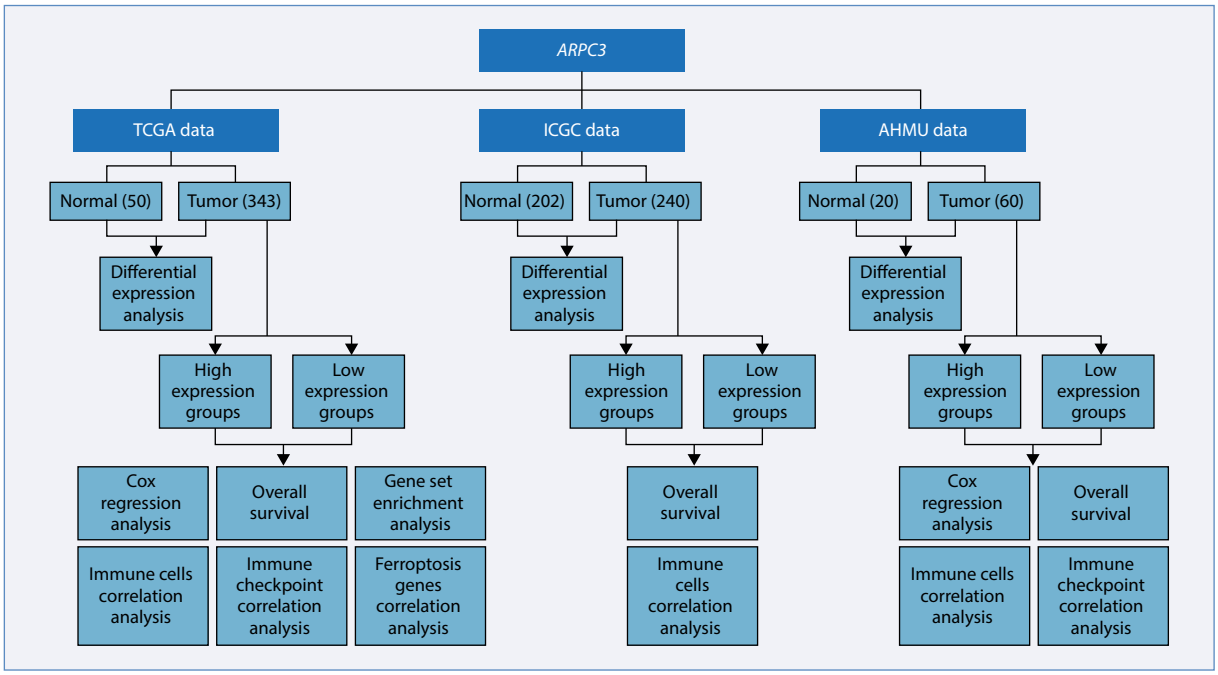

Figure 1. Flowchart of the study; AHMU — First Affiliated Hospital of Anhui Medical University; ICGC — International Cancer Genome Consortium; TCGA — The Cancer Genome Atlas

Table 1. Primer sequences of quantitative real-time polymerase chain reaction (qRT-PCR)

Genes		Primer sequences (5′-3′)
ARPC3	F	GCAATTCCAAAAGCCAAGGTG
	R	AGGCTCTCATCACTTCATCTTCC
PD-L1	F	TGGCATTTGCTGAACGCATTT
	R	TGCAGCCAGGTCTAATTGTTTT
PD-1	F	CCAGCCCCTGAAGGAGGA
	R	GCCCATTCCGCTAGGAAAGA
PD-L2	F	ACCCTGGAATGCAACTTTGAC
	R	AAGTGGCTCTTTCACGGTGTG
CTLA4	F	GCCCTGCACTCTCCTGTTTTT
	R	GGTTGCCGCACAGACTTCA
TNFRSF14	F	ACCGAGAGTCAGGACACCC
	R	AGCAAACAATGACGATGACGA
IDO1	F	GCCAGCTTCGAGAAAGAGTTG
	R	ATCCCAGAACTAGACGTGCAA
GAPDH	F	AGAAGGCTGGGGCTCATTTG
	R	AGGGGCCATCCACAGTCTC

ARPC3 — actin related protein 2/3 complex subunit 3; *CTLA4* — cytotoxic T lymphocyte-associated antigen-4; *IDO1* — indoleamine 2,3-dioxygenase 1; *PD-1* — programmed death 1; *PD-L1* — programmed death ligand 1; *PD-L2* — programmed death ligand 2; *TNFRSF14* — tumor necrosis factor receptor superfamily, member 14

are two widely recognized databases. Hepatocellular carcinoma patient sequencing data and related clinical data were downloaded. Patients with fewer than 30 days of survival and patients without clinicopathological parameters from TCGA data were excluded; thus, 343 patients were included in the analysis. ICGC data included 240 tumor samples and 202 normal tissue samples. The TCGA, ICGC, and HPA databases (https://www.proteinatlas.org/) were applied to validate the RNA and protein levels.

Survival analysis

GraphPad Prism 6 software (PRISm-6.33.5-R2, US) was used to analyze the survival results of different *ARPC3* expression groups with the Kaplan-Meier (K-M) method, and a log-rank test was performed. Clinicopathological parameters, such as age, sex, tumor diameter, tumor number, tumor envelope, tumor node metastasis classification (TNM) stage, and Barcelona Clinic Liver Cancer (BCLC) stage, were analyzed using a Cox regression model, and $p < 0.05$ was considered statistically significant.

Immunofluorescence staining

Sixty formalin-fixed paraffin-embedded (FFPE) HCC tissue samples from patients who underwent hepatobiliary surgery at AHMU were collected. Immunofluorescence staining (IF) was performed to label CD20+ B and CD3+ T cells. At 400× magnification, images of at least 3 fields were obtained for each sample. Image-Pro software (Image-Pro Plus 7.0, US) was used for counting, and the average cell count of the three regions was calculated [22].

Enrichment analysis

Gene Set Enrichment Analysis (GSEA) (https://www.gsea-msigdb.org/gsea/) is the most commonly used tool to predict molecular pathways. All TCGA tumor samples were divided into high and low *ARPC3* expression groups for Gene Ontology (GO) and Kyoto Encyclopedia of Genes and Genomes (KEGG) enrichment analyses to explore the different molecular action principles. The corresponding genes affecting specific molecular pathways were downloaded from GSEA, and $P < 0.05$ was used as the criterion for statistical significance of the results.

Analysis of immune cell infiltration

Tumor-infiltrating lymphocytes are the ultimate therapeutic target of ICIs; therefore, we used the TIMER (https://cistrome.shinyapps.io/timer/), AHMU data, and ICGC databases to analyze the relationship between *ARPC3* expression and TILs. Next, the number of TILs in each patient was assessed using the XCELL, CIBERSORT, and MCP-counter algorithms to detect the relationship between *ARPC3* and TILs.

Ferroptosis-related gene analysis

Ferroptosis in HCC immunotherapy is gradually emerging. To further study the role of *ARPC3* in immunotherapy, we downloaded 76 ferroptosis-related genes from FerrDb (http://www.zhounan.org/ferrdb/index.html) and 832 genes associated with *ARPC3* from UALCAN (http://ualcan.path.uab.edu/index.html) (Cor > 0.5). Then, Spearman analysis was performed to calculate the correlation between *ARPC3* and ferroptosis-related genes.

Statistical analysis

An unpaired t-test was performed for the expression differences of *ARPC3* using GraphPad Prism 6 software. Survival differences were expressed by the K-M curve and determined by the log-rank test. Spearman correlation analysis was used for correlation analysis. Related R packages included “pheatmap”, “timeROC”, “ggplot2”, and “GSEABase”. $P < 0.05$ was considered statistically significant.

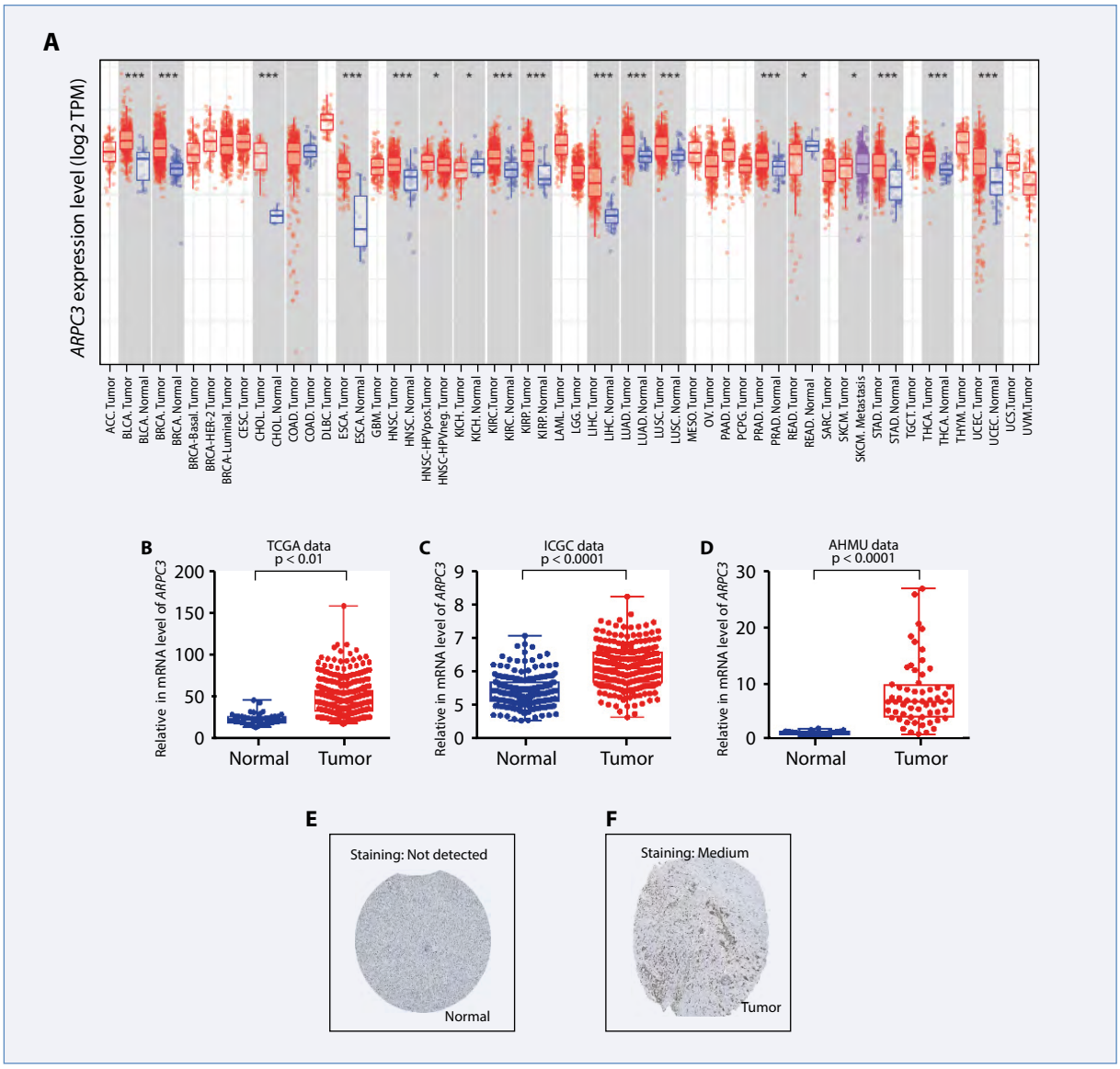

Figure 2. A. *ARPC3* expression levels in various cancer tissues determined using the TIMER analysis (notes: $p < 0.0001$ = ****, $p < 0.001$ = ***, $p < 0.01$ = **, and $p < 0.05$ = *). The differential expression of *ARPC3* in tumor and adjacent normal tissues from the following sources was mapped using GraphPad Prism 6 software: (**B**) The Cancer Genome Atlas (TCGA) data, (**C**) International Cancer Genome Consortium (ICGC) data, and (**D**) First Affiliated Hospital of Anhui Medical University (AHMU) data. Representative images of immunohistochemical staining for *ARPC3* in hepatocellular carcinoma (HCC) tissues and normal liver tissues from the Human protein atlas: (**E**) normal tissues, (**F**) tumor tissues

Results

Analysis of differences in *ARPC3* expression

ARPC3 mRNA levels differ in various cancers (e.g., HCC) (Fig. 2A). Therefore, *ARPC3* may play a crucial role in a variety of tumors. Because HCC patients are less sensitive to ICIs and targeted drugs, *ARPC3* has a high correlation with immune lymphocytes in HCC. Here, we focused on evaluating the mechanism of *ARPC3* in HCC. According to the TCGA and ICGC datasets, *ARPC3* mRNA was expressed at higher levels in HCC tissues than in normal tissues ($p < 0.0001$) (Fig. 2B, C). Subsequently, the same result was obtained through validation with the AHMU HCC dataset ($p < 0.0001$) (Fig. 2D). The immunohistochemistry results in the HPA database demonstrated that the expression of the *ARPC3* protein in HCC was also significantly upregulated (Fig. 2E, F). Thus, *ARPC3* was expressed at higher levels in HCC tissues than in normal tissues.

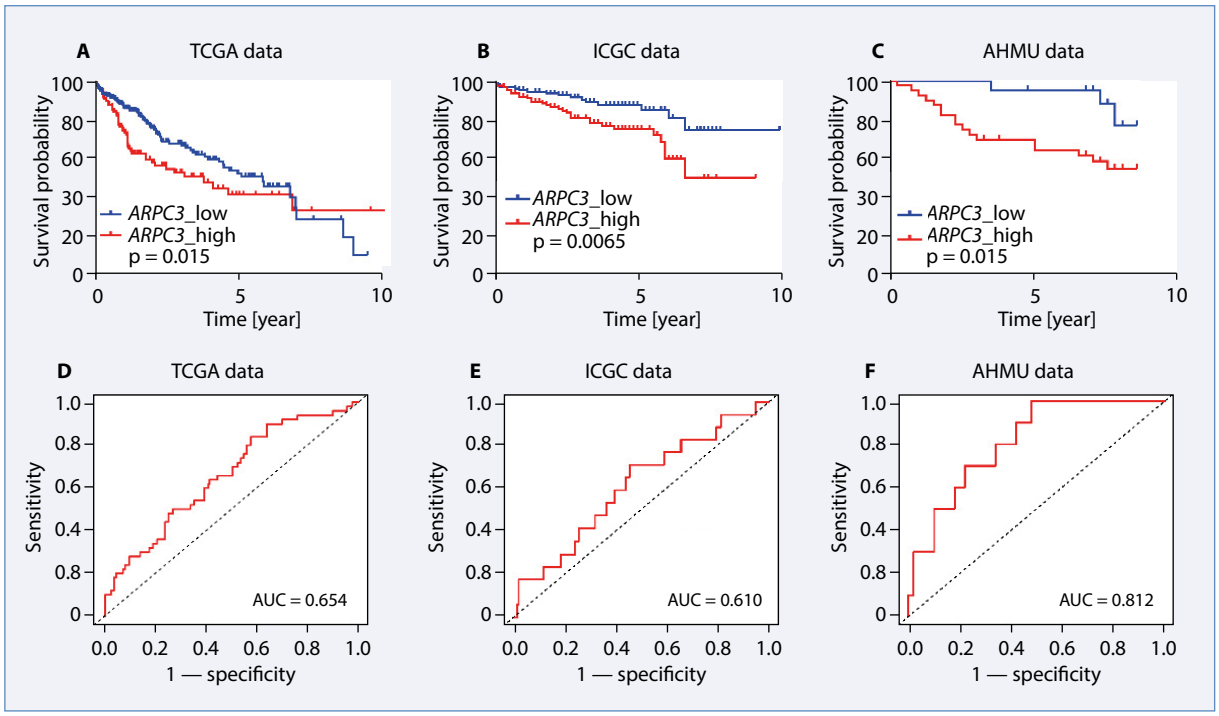

Figure 3. Kaplan-Meier (K-M) curves plotted using GraphPad Prism 6 software show overall survival (OS), and high expression of *ARPC3* was associated with a poor prognosis for patients in (**A**) The Cancer Genome Atlas (TCGA) data, (**B**) International Cancer Genome Consortium (ICGC) data, and (**C**) First Affiliated Hospital of Anhui Medical University (AHMU) data. Receiver Operating Characteristic (ROC) curves for patients with hepatocellular carcinoma (HCC) 1 year after surgery were drawn using the R package "timeROC": (**D**) TCGA, (**E**) ICGC, and (**F**) AHMU datasets; AUC — area under the curve

High *ARPC3* expression predicts shorter survival for hepatocellular carcinoma patients

First, TCGA and ICGC data were used to suggest that HCC patients with high expression of *ARPC3* had worse prognosis than those with low expression of *ARPC3* (Fig. 3A, B). Data from AHMU were used to verify the above results (Fig. 3C). In addition, the areas under the ROC curve (AUCs) 1 year after surgery were 0.654, 0.610, and 0.812, suggesting that *ARPC3* was a strong predictor of overall survival (OS) (Fig. 3D–F). Univariate and multivariate Cox regression analyses were used to determine the relationship between risk factors in the AHMU dataset and the prognosis for HCC patients. Univariate and multivariate Cox regression analyses showed that *ARPC3* ($p = 0.024$), AFP level ($p = 0.028$), tumor diameter ($p = 0.001$), and tumor capsule ($p = 0.002$) were significantly correlated with OS while tumor diameter [hazard ratio (HR) = 5.453; 95% confidence interval (CI) 2.033–14.625; $p = 0.001$], tumor capsule (HR = 5.197; 95% CI 1.877–14.386; $p = 0.002$), and *ARPC3* (HR = 4.427; 95% CI 1.012—19.371; $p = 0.048$) were independent risk factors for HCC (Tab. 2). The clinicopathological features of HCC patients are shown in Table 3. The survival distribution of HCC patients plotted using TCGA data showed that with the increase in *ARPC3* expression, the number of HCC patients who died gradually increased (Fig. 4A, B).

Enrichment analysis

Evaluation of the potential molecular mechanisms of *ARPC3* may help provide new clinical treatments. We used the TCGA dataset to perform GO and KEGG analyses to explore the relevant mechanism by which *ARPC3* regulates HCC. We selected the top 10 pathways associated with *ARPC3* and the $p < 0.05$ pathway. The results showed that upregulated expression of *ARPC3* mainly affected the immune-related pathways of HCC, which suggests that *ARPC3* may affect the prognosis for HCC patients by regulating their immune response (Fig. 4C).

Relationship between tumor-infiltrating lymphocytes and *ARPC3*

Tumor-infiltrating lymphocytes are the ultimate therapeutic target of ICIs; thus, the identification of a molecule associated with immune cells is urgently needed. TCGA data (Fig. 5A, B) and ICGC data (Fig. 6) showed that *ARPC3* was positively correlated with

Table 2. Univariate and multivariate cox regression analyses of risk factors associated with overall survival of hepatocellular carcinoma (HCC) patients in First Affiliated Hospital of Anhui Medical University (AHMU)

Variables	Univariate analysis		Multivariate analysis	
	HR (95% CI)	p value	HR (95% CI)	p value
Sex (male *vs.* female)	0.688 (0.228–2.075)	0.507		
Age (> 60 *vs.* ≤ 60)	0.618 (0.223–1.717)	0.356		
HBsAg (positive *vs.* negative)	26.303 (0.126–5505.541)	0.230		
TBil [umol/L] (> 14.3 *vs.*≤ 14.3)	1.424 (0.541–3.749)	0.474		
AFP [ng/mL] (> 7.79 *vs.* ≤ 7.79)	9.506 (1.268–71.275)	**0.028**		
CA199 [U/mL] (> 37 *vs.* ≤ 37)	1.174 (0.423–3.260)	0.758		
Liver cirrhosis	1.224 (0.482–3.110)	0.671		
Number of tumors (multiple *vs.* single)	0.800 (0.185–3.463)	0.765		
Tumor diameter [cm] (> 7.71 *vs.* ≤7.71)	4.413 (1.765–11.031)	**0.001**	5.453 (2.033–14.625)	**0.001**
Tumor capsular (no *vs.* yes)	4.478 (1.751–11.453)	**0.002**	5.197 (1.877–14.386)	**0.002**
Cell differentiation (poor/moderate *vs.* well)	1.019 (0.550–1.888)	0.952		
MVI (yes *vs.* no)	1.788 (0.679–4.706)	0.239		
BCLC (B + C *vs.* 0 + A)	1.620 (0.616–4.264)	0.328		
TNM (III + IV *vs.* I + II)	0.373 (0.050–2.798)	0.338		
ARPC3 (> 4.87 *vs.* ≤ 4.87)	5.387 (1.243–23.343)	**0.024**	4.427 (1.012–19.371)	**0.048**

AFP — alpha-fetoprotein; BCLC — Barcelona Clinic Liver Cancer; CI — confidence interval; HBsAg — hepatitis B virus surface antigen; HR — hazard ratio; MVI — microvascular invasion; TNM — tumor node metastasis classification

Table 3. Clinicopathological characteristics of 60 hepatocellular carcinoma (HCC) patients in First Affiliated Hospital of Anhui Medical University (AHMU)

Characteristics	n	[%]	Characteristics	n	[%]
Sex			Tumor diameter [cm]		
Male	50	83.3	> 7.71	17	28.3
Female	10	16.7	≤ 7.71	43	71.7
Age			Tumor capsule		
> 60	20	33.3	Yes	50	83.3
≤ 60	40	66.7	No	10	16.7
HBsAg			Cell differentiation		
Positive	52	86.7	Poor/moderate	51	85.0
Negative	8	13.3	Well	9	15.0
TBil [μmol/L]			Microvascular invasion		
> 14.3	36	60.0	Yes	35	58.3
≤ 14.3	24	40.0	No	25	41.7
AFP [ng/mL]			BCLC		
> 7.79	42	70.0	0	2	3.3
≤ 7.79	18	30.0	A	23	38.4
Liver cirrhosis			B	2	3.3
Yes	36	60.0	C	33	55.0
No	24	40.0	TNM		
Tumor number			I	27	45.0
Single	53	88.3	II	27	45.0
Multiple	7	11.7	III	2	3.3
			IV	4	6.7

AFP — alpha-fetoprotein; BCLC — Barcelona Clinic Liver Cancer; HBsAg — Hepatitis B virus surface antigen; TNM — tumor node metastasis classification

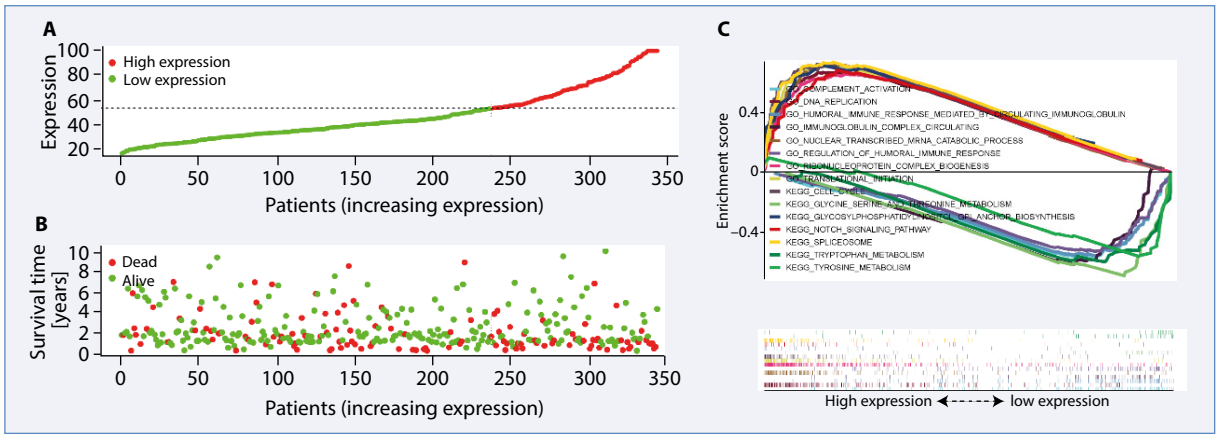

Figure 4. In The Cancer Genome Atlas (TCGA) data, the R package "ggrisk" was used to analyze the effect of the *ARPC3* expression level on the survival time and survival state of patients in TCGA; **A.** Scatter plot showing the *ARPC3* expression level from low to high; **B.** Scatter plot showing the distribution of survival time and survival state corresponding to the *ARPC3* expression level; **C.** According to the differences between *ARPC3* high expression group and low expression group, the representative hallmark term Gene Set Enrichment Analysis (GSEA) plot was drawn

the intratumor infiltration of B cells, T cells, CD4+ Th1 cells, CD4+ Th2 cells, M1 macrophages, myeloid dendritic cells, and neutrophils while it was negatively correlated with the intratumor infiltration of M2 macrophages and NK cells. The percentages of CD20+ B cells and CD3+ T cells among TILs were selectively verified by IF of AHMU FFPE sections (Fig. 7A, B), and the results also demonstrated that *ARPC3* has positive correlations with CD20+ B and CD3+ T cells (Fig. 7C, D).

Immunotherapy

In recent years, the use of ICIs in clinical treatment of tumors has greatly improved the tumor resection rate and tumor-free survival of patients. However, they have not produced ideal improvements in the ORR or progression-free survival (PFS). Therefore, using the "Pheatmap" R package, we calculated that *ARPC3* was positively correlated with immune checkpoint genes such as *PD-1, PD-L1, PD-L2, CTLA4, IDO1*, and *TNFRSF14* (Fig. 8A). Six genes were selected for qRT-PCR validation based on AHMU data, and they were positively correlated with *ARPC3* (Fig. 8B–G). These results suggest that the expression of *ARPC3* may upregulate the expression of immune checkpoints on lymphocytes and inhibit the immune function of lymphocytes.

Ferroptosis-related gene analysis

Ferroptosis is a new mode of programmed cell death that depends on iron and differs from apoptosis, necrosis, and autophagy [23], but its clinical significance and potential mechanism are still unclear. We found that *MAPK3* and *ATG7* were ferroptosis-related genes that were positively correlated with *ARPC3* (Fig. 9A). Subsequently, the correlations between *MAPK3* and *ATG7* with *ARPC3* were verified by TCGA data (Fig. 9B, C). Therefore, *ARPC3* may influence the immunotherapy response of HCC patients by influencing the expression of ferroptosis-related genes.

Discussion

The composition of TILs in the TME can reveal the mechanism of immune escape by tumor cells [24]. Moreover, the compositional nonstationary nature of the TME provides environmental support for tumor growth at different stages [25]. The GSEA results suggested that elevated expression of *ARPC3* could significantly affect immune-related pathways. Therefore, the potential role of *ARPC3* in immunotherapy was explored by investigating the relationship between *ARPC3* and TILs. Our results showed that the expression level of *ARPC3* was positively correlated with B cells, T cells, CD4+ Th1 cells, CD4+ Th2 cells, M1 macrophages, myeloid dendritic cells, and neutrophils and negatively correlated with M2 macrophages and NK cells. Based on these findings, *ARPC3* may alter the ratio of TILs in the TME and affect the ORR of HCC patients to ICIs. The potential explanation is that the bidirectional communication between tumors and TILs promotes tumor progression and metastasis (for instance, abnormal B-cell proliferation results in autoantibody production and increased expression of surface immunosuppressive ligands or cytokines, which

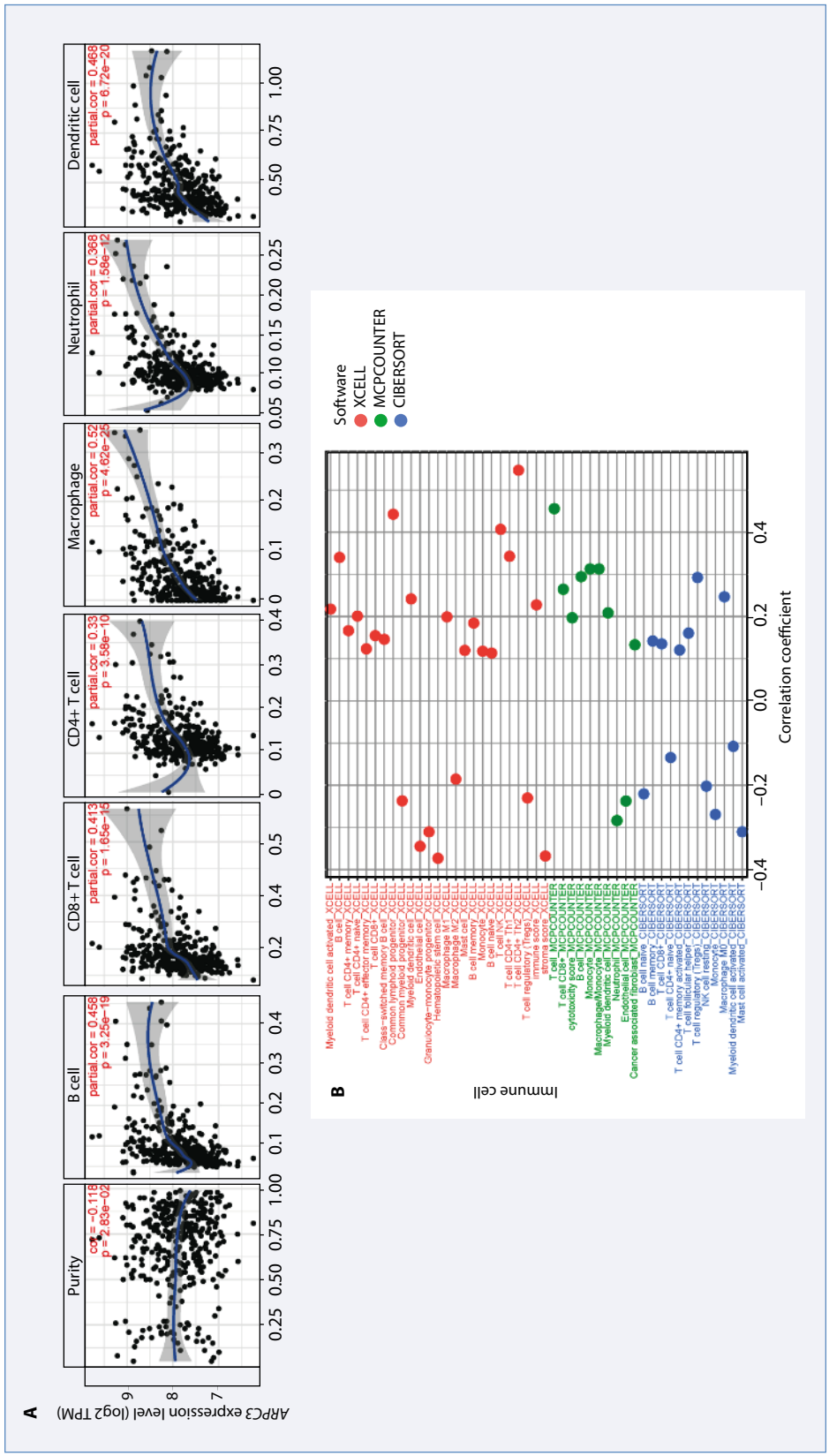

Figure 5. Correlation analysis between *ARPC3* expression and levels of infiltrating immune cells in hepatocellular carcinoma (HCC) using (**A**) TIMER and (**B**) the R package "ggtext" based on XCELL, MCP-counter and CIBERSORT algorithm

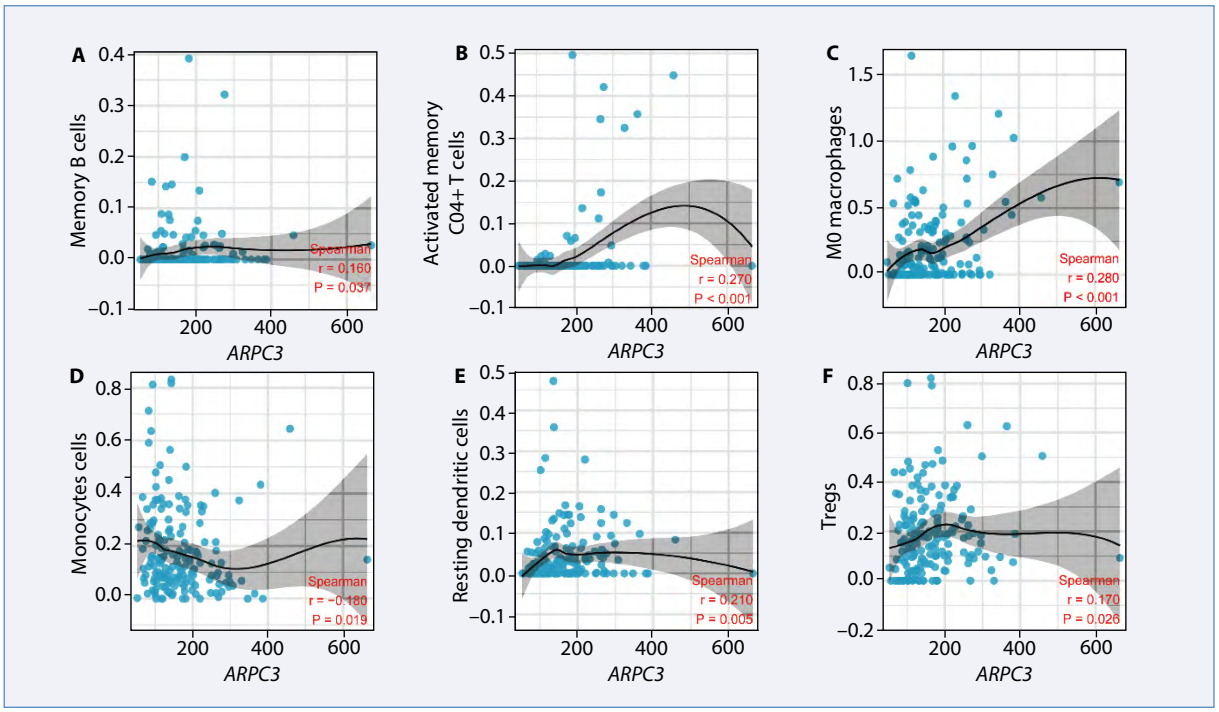

Figure 6. Correlation analysis between *ARPC3* expression and levels of infiltrating immune cells in International Cancer Genome Consortium (ICGC) hepatocellular carcinoma (HCC); **A.** Memory B cells; **B.** Activated memory CD4+ T cells; **C.** M0 macrophages; **D.** Monocytes; **E.** Resting dendritic cells; **F.** Tregs

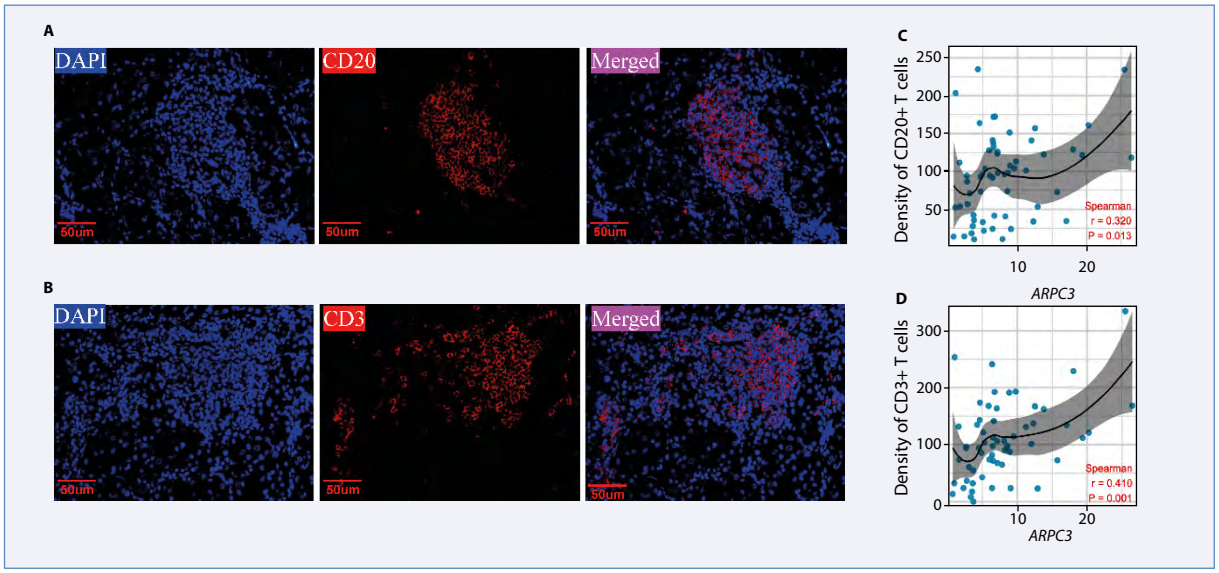

Figure 7. Representative images of immunofluorescence staining for CD20 (red) and CD3 (red) and 4′,6-diamidino-2-phenylindole (DAPI) nuclear staining (blue) in First Affiliated Hospital of Anhui Medical University (AHMU) data-hepatocellular carcinoma (HCC); **A.** CD20+ B cells and (B) CD3+ T cells. 400× magnification; **C, D.** Scatter plot showing the correlation between *ARPC3* and CD20+ B cell density [number of cells/high power field (HP)] and CD3+ T cell density (number of cells/HP)

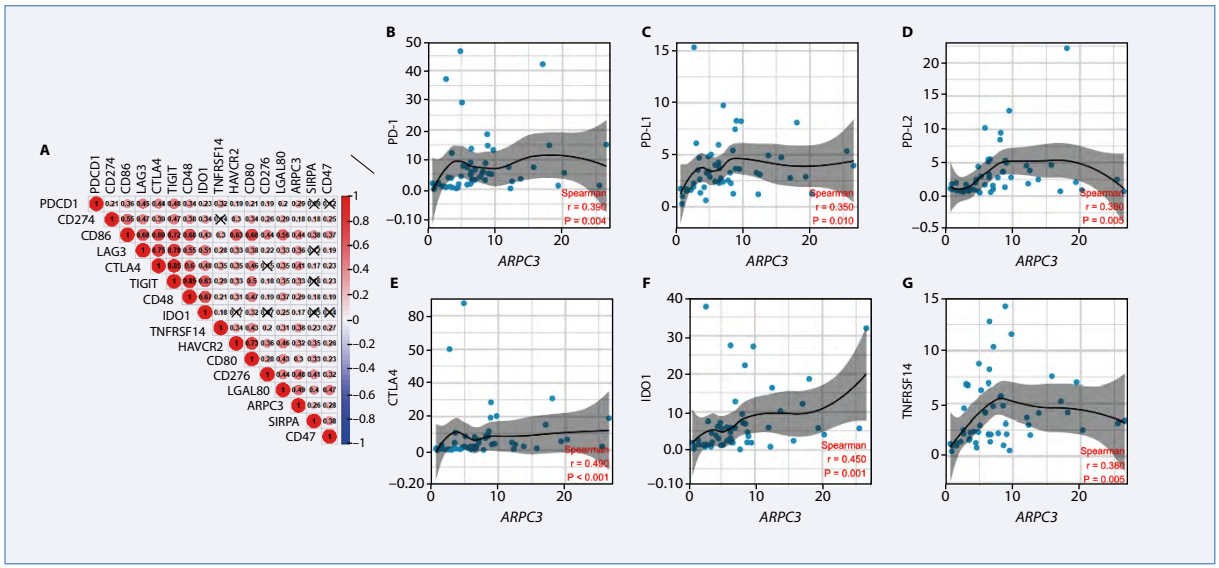

Figure 8. A. The R package "Pheatmap" was used to draw a heatmap of the association of *ARPC3* expression with immune checkpoints; **B–G.** Scatter plot showing the correlation between immune checkpoints and *ARPC3* verified by r quantitative real-time polymerase chain reaction (qRT-PCR) based on AHMU data

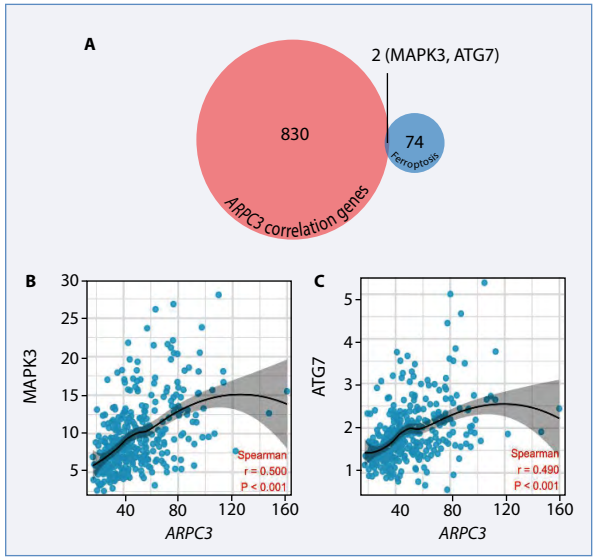

Figure 9. A. Venn diagram showing *ARPC3*-related genes and ferroptosis-related genes; **B, C.** Scatter plots showing the correlations between *ARPC3* with *MAPK3* and *ATG7*

promote the immune escape of tumor cells) [26]. Tumor-associated macrophages (TAMs) are considered a key factor in the TME and tumor invasiveness [25]. The role of macrophages in promoting cancer is related to the polarization of M2 macrophages while interferon-γ and other factors stimulate the activation of M1 polarized macrophages that produce proinflammatory and immune-stimulating factors (e.g., IL-12 or TNF-α) [27]. M1 macrophages activate *STAT3* by secreting IL-35 and promote the epithelial-mesenchymal transition (EMT) of HCC cells [28]. Exosomes secreted by HCC cells stimulate the polarization of M2 macrophages and promote the migration, invasion, and EMT of HCC [29]. Increased numbers of myeloid-derived suppressor cells in the TME promote the growth of tumor cells by increasing tumor angiogenesis and the number of Tregs as well as enhancing the Th2 response [30]. Based on accumulating evidence, inflammation is necessary for the initiation and progression of HCC, and HCC cells release chemokine C-X-C motif chemokine ligand *(CXCL)-2, CXCL8*, and *CCL25* to increase the neutrophil ratio in the TME, forming an immunosuppressive microenvironment and leading to immune escape of tumor cells [31, 32]. Reduction in the number of NK cells and NK-cell dysfunction are observed in tumor tissues, and the density of NK cells is positively correlated with a better prognosis for patients with liver cancer [33]. This finding may be related to the strong antitumor activity of NK cells, which directly lyse cells and/or produce cytokines [34]. Therefore, NK-cell-based immunotherapy may improve the inhibition of tumor growth by NK cells and be conducive to the treatment of HCC [35]. In conclusion, *ARPC3* may affect the efficacy of immunotherapy in HCC patients by influencing the composition of the TME.

In recent years, ICIs (e.g., pembrolizumab) and multitarget drugs (e.g., sorafenib) have become important neoadjuvant therapies for tumors, but the ORR to anti-PD-L1/PD-1 therapy of HCC patients is relatively low. The response rate of patients to ICIs can be improved by regulating *PD-L1*-related signaling pathways [36].

The results of our study indicate that several immune checkpoint genes, including *PD-1* and *PD-L1*, were positively correlated with *ARPC3*. *PD-L1* and *CTLA-4* are highly expressed in dendritic cells (DCs) and B cells in HCC and downregulate the T-cell-mediated immune response through immunosuppression [37]. Therefore, patients with high *ARPC3* expression may be in an immunosuppressive state that is insensitive to ICIs and targeted drugs.

Ferroptosis is a potential cell death pathway and target for HCC treatment. As shown in our study, *MAPK3* and *ATG7* are ferroptosis-related genes that are positively correlated with *ARPC3*. Sorafenib, a promoter of ferroptosis, causes the accumulation of reactive oxygen species by inhibiting system XC-, leading to the depletion of intracellular glutathione, ferroptosis, and an increased response rate of patients to sorafenib [23, 38, 39]. Sorafenib alters the methylation level of *MAPK3*, a gene related to tumor growth and metastasis in HCC, and inhibits tumor growth and metastasis [40, 41]. *ATG7* is an autophagy-related protein, and its knockdown inhibits ferritin degradation, lipid peroxidation, and ferroptosis, which can improve the ORR of patients to ICIs and reduce the drug resistance rate [42, 43]. Therefore, ICIs or targeted drugs combined with ferroptosis therapy may be beneficial to prolong survival of HCC patients with high expression of *ARPC3* in the immunosuppressed state.

Conclusions

Our study found that *ARPC3* is an independent risk factor for HCC, and the higher the expression of *ARPC3*, the worse the prognosis for HCC patients. In addition, *ARPC3* may affect the balance of the tumor microenvironment by regulating the TIL ratio, resulting in failure of immunotherapy in HCC patients.

Article Information and Declarations

Data availability statement
The datasets generated and/or analyzed during the current study are available in the TCGA and ICGC repositories.

Ethics statement
This study has been approved by the Ethics Committee of the First Affiliated Hospital of Anhui Medical University.

Author contributions
Y.S.: designed the whole study, drafted the manuscript, made the relevant edits to the manuscript; J.L.: performed the qRT-PCR and immunofluorescence staining analysis; Z.L.: conducted the statistical analysis, performed the qRT-PCR and immunofluorescence staining analysis; Y.Q.: designed the whole study, drafted the manuscript, revised the manuscript.

Funding
None.

Acknowledgments
None.

Conflict of interest
The authors have no conflicts of interest to disclose.

Supplementary material
None.

References

1. Rimassa L, Pressiani T, Merle P, et al. Systemic Treatment Options in Hepatocellular Carcinoma. Liver Cancer. 2019; 8(6): 427–446, doi: 10.1159/000499765, indexed in Pubmed: 31799201.
2. Sung H, Ferlay J, Siegel RL, et al. Global Cancer Statistics 2020: GLOBOCAN Estimates of Incidence and Mortality Worldwide for 36 Cancers in 185 Countries. CA Cancer J Clin. 2021; 71(3): 209–249, doi: 10.3322/caac.21660, indexed in Pubmed: 33538338.
3. Bruix J, Gores GJ, Mazzaferro V. Hepatocellular carcinoma: clinical frontiers and perspectives. Gut. 2014; 63(5): 844–855, doi: 10.1136/gutjnl-2013-306627, indexed in Pubmed: 24531850.
4. Bruix J, Han KH, Gores G, et al. Liver cancer: Approaching a personalized care. J Hepatol. 2015; 62(1 Suppl): S144–S156, doi: 10.1016/j.jhep.2015.02.007, indexed in Pubmed: 25920083.
5. Wang L, Wang FS. Clinical immunology and immunotherapy for hepatocellular carcinoma: current progress and challenges. Hepatol Int. 2019; 13(5): 521–533, doi: 10.1007/s12072-019-09967-y, indexed in Pubmed: 31352593.
6. van Kempen LC, Ruiter DJ, van Muijen GNP, et al. The tumor microenvironment: a critical determinant of neoplastic evolution. Eur J Cell Biol. 2003; 82(11): 539–548, doi: 10.1078/0171-9335-00346, indexed in Pubmed: 14703010.
7. Dong H, Yang Y, Gao C, et al. Lactoferrin-containing immunocomplex mediates antitumor effects by resetting tumor-associated macrophages to M1 phenotype. J Immunother Cancer. 2020; 8(1), doi: 10.1136/jitc-2019-000339, indexed in Pubmed: 32217759.
8. Zhang H, Liu H, Shen Z, et al. Tumor-infiltrating Neutrophils is Prognostic and Predictive for Postoperative Adjuvant Chemotherapy Benefit in Patients With Gastric Cancer. Ann Surg. 2018; 267(2): 311–318, doi: 10.1097/SLA.0000000000002058, indexed in Pubmed: 27763900.
9. Zhu H, Wang G, Zhu H, et al. ITGA5 is a prognostic biomarker and correlated with immune infiltration in gastrointestinal tumors. BMC Cancer. 2021; 21(1): 269, doi: 10.1186/s12885-021-07996-1, indexed in Pubmed: 33711961.
10. Kinoshita T, Muramatsu R, Fujita T, et al. Prognostic value of tumor-infiltrating lymphocytes differs depending on histological type and smoking habit in completely resected non-small-cell lung cancer. Ann Oncol. 2016; 27(11): 2117–2123, doi: 10.1093/annonc/mdw319, indexed in Pubmed: 27502728.
11. Dieci MV, Radosevic-Robin N, Fineberg S, et al. International Immuno-Oncology Biomarker Working Group on Breast Cancer. Update on tumor-infiltrating lymphocytes (TILs) in breast cancer, including recommendations to assess TILs in residual disease after neoadjuvant therapy and in carcinoma in situ: A report of the International Immuno-Oncology Biomarker Working Group on Breast Cancer. Semin Cancer Biol. 2018; 52(Pt 2): 16–25, doi: 10.1016/j.semcancer.2017.10.003, indexed in Pubmed: 29024776.
12. Wang YQ, Chen YP, Zhang Yu, et al. Prognostic significance of tumor-infiltrating lymphocytes in nondisseminated nasopharyngeal carcinoma: A large-scale cohort study. Int J Cancer. 2018; 142(12): 2558–2566, doi: 10.1002/ijc.31279, indexed in Pubmed: 29377121.

13. Kang HJ, Oh JH, Chun SM, et al. Immunogenomic landscape of hepatocellular carcinoma with immune cell stroma and EBV-positive tumor-infiltrating lymphocytes. J Hepatol. 2019; 71(1): 91–103, doi: 10.1016/j.jhep.2019.03.018, indexed in Pubmed: 30930222.
14. Pötzsch M, Berg E, Hummel M, et al. Better prognosis of gastric cancer patients with high levels of tumor infiltrating lymphocytes is counteracted by PD-1 expression. Oncoimmunology. 2020; 9(1): 1824632, doi: 10.1080/2162402X.2020.1824632, indexed in Pubmed: 33101772.
15. Zhang L, Zhang Y, Lei Y, et al. Proline-rich 11 (PRR11) drives F-actin assembly by recruiting the actin-related protein 2/3 complex in human non-small cell lung carcinoma. J Biol Chem. 2020; 295(16): 5335–5349, doi: 10.1074/jbc.RA119.012260, indexed in Pubmed: 32169900.
16. Markwell SM, Ammer AG, Interval ET, et al. Cortactin Phosphorylation by Casein Kinase 2 Regulates Actin-Related Protein 2/3 Complex Activity, Invadopodia Function, and Tumor Cell Invasion. Mol Cancer Res. 2019; 17(4): 987–1001, doi: 10.1158/1541-7786.MCR-18-0391, indexed in Pubmed: 30610108.
17. Yae K, Keng VW, Koike M, et al. Sleeping beauty transposon-based phenotypic analysis of mice: lack of Arpc3 results in defective trophoblast outgrowth. Mol Cell Biol. 2006; 26(16): 6185–6196, doi: 10.1128/MCB.00018-06, indexed in Pubmed: 16880528.
18. Mu J, Zhang Y, Hu Y, et al. The role of viral protein Ac34 in nuclear relocation of subunits of the actin-related protein 2/3 complex. Virol Sin. 2016; 31(6): 480–489, doi: 10.1007/s12250-016-3912-4, indexed in Pubmed: 27900558.
19. Zhou K, Muroyama A, Underwood J, et al. Actin-related protein2/3 complex regulates tight junctions and terminal differentiation to promote epidermal barrier formation. Proc Natl Acad Sci U S A. 2013; 110(40): E3820–E3829, doi: 10.1073/pnas.1308419110, indexed in Pubmed: 24043783.
20. Zhang C, Wu S, Yang XD, et al. Identification of Key Genes for Hepatitis Delta Virus-Related Hepatocellular Carcinoma by Bioinformatics Analysis. Turk J Gastroenterol. 2021; 32(2): 169–177, doi: 10.5152/tjg.2020.191003, indexed in Pubmed: 33960941.
21. Rai A, Greening DW, Xu R, et al. Exosomes Derived from the Human Primary Colorectal Cancer Cell Line SW480 Orchestrate Fibroblast-Led Cancer Invasion. Proteomics. 2020; 20(14): e2000016, doi: 10.1002/pmic.202000016, indexed in Pubmed: 32438511.
22. Garnelo M, Tan A, Her Z, et al. Interaction between tumour-infiltrating B cells and T cells controls the progression of hepatocellular carcinoma. Gut. 2017; 66(2): 342–351, doi: 10.1136/gutjnl-2015-310814, indexed in Pubmed: 26669617.
23. Wang Qi, Guo Y, Wang W, et al. RNA binding protein DAZAP1 promotes HCC progression and regulates ferroptosis by interacting with SLC7A11 mRNA. Exp Cell Res. 2021; 399(1): 112453, doi: 10.1016/j.yexcr.2020.112453, indexed in Pubmed: 33358859.
24. Li Bo, Severson E, Pignon JC, et al. Comprehensive analyses of tumor immunity: implications for cancer immunotherapy. Genome Biol. 2016; 17(1): 174, doi: 10.1186/s13059-016-1028-7, indexed in Pubmed: 27549193.
25. Wan PKT, Ryan AJ, Seymour LW. Beyond cancer cells: Targeting the tumor microenvironment with gene therapy and armed oncolytic virus. Mol Ther. 2021; 29(5): 1668–1682, doi: 10.1016/j.ymthe.2021.04.015, indexed in Pubmed: 33845199.
26. Hiss S, Eckstein M, Segschneider P, et al. Tumour-Infiltrating Lymphocytes (TILs) and PD-L1 Expression Correlate with Lymph Node Metastasis, High-Grade Transformation and Shorter Metastasis-Free Survival in Patients with Acinic Cell Carcinoma (AciCC) of the Salivary Glands. Cancers (Basel). 2021; 13(5), doi: 10.3390/cancers13050965, indexed in Pubmed: 33669038.
27. Wu J, Gao W, Tang Q, et al. M2 Macrophage-Derived Exosomes Facilitate HCC Metastasis by Transferring α β Integrin to Tumor Cells. Hepatology. 2021; 73(4): 1365–1380, doi: 10.1002/hep.31432, indexed in Pubmed: 32594528.
28. He Y, Pei JH, Li XQ, et al. IL-35 promotes EMT through STAT3 activation and induces MET by promoting M2 macrophage polarization in HCC. Biochem Biophys Res Commun. 2021; 559: 35–41, doi: 10.1016/j.bbrc.2021.04.050, indexed in Pubmed: 33932898.
29. Wang LP, Lin J, Ma XQ, et al. Exosomal DLX6-AS1 from hepatocellular carcinoma cells induces M2 macrophage polarization to promote migration and invasion in hepatocellular carcinoma through microRNA-15a-5p/CXCL17 axis. J Exp Clin Cancer Res. 2021; 40(1): 177, doi: 10.1186/s13046-021-01973-z, indexed in Pubmed: 34039401.
30. Kalathil SG, Wang K, Hutson A, et al. Tivozanib mediated inhibition of c-Kit/SCF signaling on Tregs and MDSCs and reversal of tumor induced immune suppression correlates with survival of HCC patients. Oncoimmunology. 2020; 9(1): 1824863, doi: 10.1080/2162402X.2020.1824863, indexed in Pubmed: 33101775.
31. Xu X, Ye L, Zhang Qi, et al. Group-2 Innate Lymphoid Cells Promote HCC Progression Through CXCL2-Neutrophil-Induced Immunosuppression. Hepatology. 2021; 74(5): 2526–2543, doi: 10.1002/hep.31855.
32. Zhu Q, Pan QZ, Zhong AL, et al. Annexin A3 upregulates the infiltrated neutrophil-lymphocyte ratio to remodel the immune microenvironment in hepatocellular carcinoma. Int Immunopharmacol. 2020; 89(Pt A): 107139, doi: 10.1016/j.intimp.2020.107139, indexed in Pubmed: 33191179.
33. Sun H, Xu J, Huang Q, et al. Reduced CD160 Expression Contributes to Impaired NK-cell Function and Poor Clinical Outcomes in Patients with HCC. Cancer Res. 2018; 78(23): 6581–6593, doi: 10.1158/0008-5472.CAN-18-1049, indexed in Pubmed: 30232222.
34. Shin S, Kim M, Lee SJ, et al. Trichostatin A Sensitizes Hepatocellular Carcinoma Cells to Enhanced NK Cell-mediated Killing by Regulating Immune-related Genes. Cancer Genomics Proteomics. 2017; 14(5): 349–362, doi: 10.21873/cgp.20045, indexed in Pubmed: 28871002.
35. Tao L, Wang S, Yang L, et al. Reduced Siglec-7 expression on NK cells predicts NK cell dysfunction in primary hepatocellular carcinoma. Clin Exp Immunol. 2020; 201(2): 161–170, doi: 10.1111/cei.13444, indexed in Pubmed: 32319079.
36. Yan Y, Zheng L, Du Q, et al. Interferon regulatory factor 1 (IRF-1) and IRF-2 regulate PD-L1 expression in hepatocellular carcinoma (HCC) cells. Cancer Immunol Immunother. 2020; 69(9): 1891–1903, doi: 10.1007/s00262-020-02586-9, indexed in Pubmed: 32377817.
37. Zhou G, Sprengers D, Boor PPC, et al. Antibodies Against Immune Checkpoint Molecules Restore Functions of Tumor-Infiltrating T Cells in Hepatocellular Carcinomas. Gastroenterology. 2017; 153(4): 1107–1119.e10, doi: 10.1053/j.gastro.2017.06.017, indexed in Pubmed: 28648905.
38. Li Y, Xia J, Shao F, et al. Sorafenib induces mitochondrial dysfunction and exhibits synergistic effect with cysteine depletion by promoting HCC cells ferroptosis. Biochem Biophys Res Commun. 2021; 534: 877–884, doi: 10.1016/j.bbrc.2020.10.083, indexed in Pubmed: 33162029.
39. Deng T, Hu B, Jin C, et al. A novel ferroptosis phenotype-related clinical-molecular prognostic signature for hepatocellular carcinoma. J Cell Mol Med. 2021; 25(14): 6618–6633, doi: 10.1111/jcmm.16666, indexed in Pubmed: 34085405.
40. Qin Z, Xiang C, Zhong F, et al. Transketolase (TKT) activity and nuclear localization promote hepatocellular carcinoma in a metabolic and a non-metabolic manner. J Exp Clin Cancer Res. 2019; 38(1): 154, doi: 10.1186/s13046-019-1131-1, indexed in Pubmed: 30971297.
41. Abeni E, Salvi A, Marchina E, et al. Sorafenib induces variations of the DNA methylome in HA22T/VGH human hepatocellular carcinoma-derived cells. Int J Oncol. 2017; 51(1): 128–144, doi: 10.3892/ijo.2017.4019, indexed in Pubmed: 28560380.
42. Hou W, Xie Y, Song X, et al. Autophagy promotes ferroptosis by degradation of ferritin. Autophagy. 2016; 12(8): 1425–1428, doi: 10.1080/15548627.2016.1187366, indexed in Pubmed: 27245739.
43. Zhou B, Liu J, Kang R, et al. Ferroptosis is a type of autophagy-dependent cell death. Semin Cancer Biol. 2020; 66: 89–100, doi: 10.1016/j.semcancer.2019.03.002, indexed in Pubmed: 30880243.